Edge dark states of dissipative dynamics in topological insulators

Jing Sun(孙静)[1], Fei Yang(杨飞)[2], Jing He(何敬)[1,†], and Ya-Jie Wu(吴亚杰)[3,‡]

[1] *College of Physics and Hebei Advanced Thin Film Laboratory, Hebei Normal University, Shijiazhuang* 050024, *China*
[2] *State Key Laboratory of Low Dimensional Quantum Physics, Department of Physics, Tsinghua University, Beijing* 100084, *China*
[3] *School of Sciences, Xi'an Technological University, Xi'an* 710032, *China*

(Received 2 October 2025; revised manuscript received 18 November 2025; accepted manuscript online 2 December 2025)

The study of topological phases in non-Hermitian systems has become a key area in condensed matter physics, providing a deep understanding of open quantum systems with dissipation. In this work, we study edge dark states (EDSs) in dissipative topologically nontrivial insulators, i.e., the dissipative Haldane model and the dissipative Kane–Mele model on a honeycomb lattice. By deriving a non-Hermitian damping matrix X from the Lindblad master equation, we characterize the system's dissipative dynamics through its Liouvillian spectrum. Numerical calculations demonstrate that EDSs, marked by vanishing imaginary parts in the spectrum ($\mathrm{Im}(\lambda)=0$), emerge as topologically protected modes localized at the system's edges. These states remain robust even in the presence of nonzero Hamiltonian contributions, contrary to previous studies showing that such protection required purely dissipative systems. We introduce a double damping matrix $\tilde{X}=\mathrm{diag}(X,X^*)$ to further demonstrate the stability of EDSs against perturbations. This work highlights the interplay between non-Hermitian topology and dissipative dynamics, paving the way for exploring novel dissipative topological phenomena.

Keywords: edge dark states, dissipative dynamics, topological insulators, open system

PACS: 03.65.Yz, 03.65.Vf, 73.43.–f

DOI: 10.1088/1674-1056/ae2675 **CSTR:** 32038.14.CPB.ae2675

1. Introduction

The search for topologically nontrivial phases has been an important goal in condensed matter physics. Decades ago, researchers discovered a variety of novel quantum states in topological Hermitian systems, such as topological insulators,[1–5] topological superconductors,[6–9] topological orders,[10–13] and higher-order topological insulators.[14–19] Furthermore, with lattice symmetries taken into account, topological crystalline insulators have also been proposed.[20,21] These topological states exhibit bulk–boundary correspondence. Topological materials with nontrivial bulk topology would host protected gapless states at their edges or surfaces.[4,14–17,22] These boundary states are robust against certain perturbations due to their bulk topology. The study of these topologically nontrivial states has not only deepened our understanding of quantum phases of matter but also opened up new avenues for technological applications, particularly in the area of spintronics and quantum computation.

In quantum mechanics, if the physical observables have real eigenvalues and their eigenstates form a complete basis, it is required that the plural Hamiltonians for the systems are Hermitian. In recent condensed matter physics, the dynamical properties of open quantum systems provide new insights. Under certain conditions, the open quantum system can be described by a non-Hermitian (NH) Hamiltonian H with $H\neq H^\dagger$. It can describe the system experiencing dissipation associated with gain and loss in atomic, molecular, and optical physics.[23,24] The breakdown of Hermiticity in the Hamiltonian leads to novel and deeper physics, such as PT-symmetry, exceptional points (EPs), the non-Hermitian skin effect, novel non-equilibrium behaviors, and the breakdown of bulk–boundary correspondence.[25–33]

The influence of non-Hermiticity on the system's topological properties has drawn considerable attention.[34–36] Nevertheless, it is often difficult to solve most of these systems analytically, especially when interactions are present. However, one solvable case is the open free fermionic system, where the dissipative dynamics are fully governed by a non-Hermitian single-particle damping matrix X that incorporates both the system Hamiltonian and dissipation. The dynamical properties of these dissipative systems are characterized by the complex spectra (or Lindbladian spectra) of the damping matrix X. Two types of special topological edge modes exist in the dissipative system — edge zero-frequency modes and edge dark states (EDSs). The edge zero-frequency modes serve as a dynamical fingerprint of topological order, inducing distinct dissipation characteristics between the bulk and boundary.[37] Reference [38] revealed that the topological phenomena in the dissipative dynamics of quadratic open fermionic systems can be understood by applying the 38-fold way to the topological classification of the complex spectrum of X (or the Lindbladian spectrum), where the symmetry of X plays a central role.

†Corresponding author. E-mail: jhe@hebtu.edu.cn
‡Corresponding author. E-mail: wuyajie@xatu.edu.cn

© 2026 Chinese Physical Society and IOP Publishing Ltd. All rights, including for text and data mining, AI training, and similar technologies, are reserved.

CPB Online In-press

Edge dark states as quantum states in open free fermionic systems have been studied in many cases.[39,40] However, earlier research primarily concentrated on purely dissipative systems, where the EDSs lose robustness when Hamiltonian contributions are present. In this work we study the EDSs in dissipative Haldane and Kane–Mele models, where both Hamiltonian and dissipation coexist on the honeycomb lattice. By numerical calculations, we find that EDSs are topologically protected by the double damping matrix $\tilde{X} = \mathrm{diag}\,(X, X^*)$, and they remain robust even when the Hamiltonian is taken into account. Moreover, the time evolution of occupation numbers indicates that the EDSs can cause chirality interruption in damped oscillatory dynamics. In the topological phase, the edge zero-frequency modes are gradually suppressed as the dissipation strength increases.

This work is organized as follows. In Section 2, we first introduce the dissipative Haldane model and analyze its damping dynamics, followed by a systematic investigation of EDSs in this framework. In Section 3, we investigate the EDSs in the dissipative Kane–Mele model. Finally, the conclusions and discussions are given in Section 4.

2. Edge dark states in the dissipative Haldane model

2.1. Dissipative Haldane model and the damping dynamics

The Haldane model is the first theoretical model to achieve the quantum Hall effect without an external magnetic field.[41] It breaks the time-reversal symmetry by the next-nearest neighbor hopping with a complex phase φ, where the positive phase is gained with clockwise hopping in the honeycomb plaquette. Its Bloch Hamiltonian is written as

$$h_{\mathrm{H}}(\boldsymbol{k}) = (h_0\sigma_0 + h_x\sigma_x + h_y\sigma_y + h_z\sigma_z), \tag{1}$$

where

$$h_0 = -2t'\cos\varphi(\cos\boldsymbol{k}\cdot\boldsymbol{a}_1 + \cos\boldsymbol{k}\cdot\boldsymbol{a}_2 + \cos\boldsymbol{k}\cdot\boldsymbol{a}_3), \tag{2}$$

$$h_x = -t(\cos\boldsymbol{k}\cdot\boldsymbol{\delta}_1 + \cos\boldsymbol{k}\cdot\boldsymbol{\delta}_2 + \cos\boldsymbol{k}\cdot\boldsymbol{\delta}_3), \tag{3}$$

$$h_y = -t(\sin\boldsymbol{k}\cdot\boldsymbol{\delta}_1 + \sin\boldsymbol{k}\cdot\boldsymbol{\delta}_2 + \sin\boldsymbol{k}\cdot\boldsymbol{\delta}_3), \tag{4}$$

$$h_z = -2t'\sin\varphi(-\sin\boldsymbol{k}\cdot\boldsymbol{a}_1 + \sin\boldsymbol{k}\cdot\boldsymbol{a}_2 + \sin\boldsymbol{k}\cdot\boldsymbol{a}_3) + m. \tag{5}$$

Here, the Pauli matrices $\sigma_{x,y,z}$ and the identity matrix σ_0 act on the sublattice space with the sublattices A and B. t, t' and m are the nearest, next-nearest neighbor hopping amplitudes and the on-site staggered potential. $\boldsymbol{\delta}_{1,2,3}$ denote the vectors between the nearest neighbor sites, which are $\boldsymbol{\delta}_1 = a_0\left(\frac{1}{2}, \frac{\sqrt{3}}{2}\right)$, $\boldsymbol{\delta}_2 = a_0\left(\frac{1}{2}, -\frac{\sqrt{3}}{2}\right)$ and $\boldsymbol{\delta}_3 = a_0(-1, 0)$. $\boldsymbol{a}_1 = \boldsymbol{\delta}_1 - \boldsymbol{\delta}_3$, $\boldsymbol{a}_2 = \boldsymbol{\delta}_3 - \boldsymbol{\delta}_2$ and $\boldsymbol{a}_3 = \boldsymbol{\delta}_2 - \boldsymbol{\delta}_1$ are the vectors between the next-nearest neighbor sites, respectively. a_0 is the lattice constant and is set to be unit. Hereafter in this work, we take $\varphi = \pi/2$, then $h_0 = 0$. There is a topological phase transition at $3\sqrt{3}t' = m$. If $3\sqrt{3}t' > m$, the system enters a quantum anomalous Hall phase (QAH) characterized by the Chern number $C = 1$, while if $3\sqrt{3}t' < m$, the system becomes a normal trivial insulator. Here, we have set $t > 0$, $t' > 0$ and $m > 0$.

In general, solving open systems is extremely difficult because there are exchanges of particles and energy between the system and the environment. Therefore, in many cases we usually carry out approximation treatments. Fortunately, the Hamiltonian of an open system of free fermions is a quadratic form of fermionic operators, and its Lindblad operators (dissipation) are linear forms of fermionic operators. We can use the single-particle correlation function C to characterize the time evolution of such systems and give the definition of the Liouvillian spectrum, so as to study the dynamical effects related to non-Hermiticity and topological structures.

For an open system of free fermions, its time evolution can be written in the form of the Lindblad master equation as[42–45]

$$\frac{\mathrm{d}}{\mathrm{d}t}\rho = -\mathrm{i}\,[H_{\mathrm{H}}, \rho] + \sum_j \left(2L_j^\dagger \rho L_j - \left\{L_j^\dagger L_j, \rho\right\}\right),$$

where ρ is the density operator, H_{H} is the Hamiltonian for the Haldane model, which corresponds to the unitary evolution of the system. The Lindblad operator $\left(L_j^\dagger, L_j\right)$ represents the dissipation caused by the Markovian bath corresponding to the non-unitary evolution of the system with

$$L_j^{\mathrm{g}} = \sum_s D_{j,s}^{\mathrm{g}} c_{j,s}^\dagger, \quad L_j^{\mathrm{l}} = \sum_s D_{j,s}^{\mathrm{l}} c_{j,s}. \tag{6}$$

Here j denotes the position of the unit cell and s denotes the internal degrees of freedom. The g and l represent dissipation of gain and loss. $D_{j,s}^{\mathrm{g/l}}$ represents the coupling strength with the environment. The time evolution process of the density matrix ρ is controlled by two parts, i.e., unitary dynamics and non-unitary dynamics. The definition of the single-particle correlation function is $C_{ij} = \mathrm{Tr}\left(\rho c_i^\dagger c_j\right)$.

Based on the anticommutation relation for fermionic operators, the time evolution equation for the single-particle correlation function is given by

$$\begin{aligned} \mathrm{i}\frac{\mathrm{d}}{\mathrm{d}t}C &= -[h^{\mathrm{T}}, C] - \mathrm{i}\left\{M_{\mathrm{g}} + M_{\mathrm{l}}^{\mathrm{T}}, C\right\} + 2\mathrm{i}M_{\mathrm{g}} \\ &= XC - CX^\dagger + 2\mathrm{i}M_{\mathrm{g}}, \end{aligned} \tag{7}$$

where in real space $H_{\mathrm{H}} = \sum_{i,j} c_i^\dagger h_{ij} c_j$, M_{g} and M_{l} represent the dissipation caused by gain and loss with

$$(M_{\mathrm{g}})_{ij} = \sum_s D_{i,s}^{\mathrm{g}^*} D_{j,s}^{\mathrm{g}}, \tag{8}$$

$$(M_{\mathrm{l}})_{ij} = \sum_s D_{i,s}^{\mathrm{l}^*} D_{j,s}^{\mathrm{l}}. \tag{9}$$

X is the damping matrix, namely, a NH single-particle matrix. It consists of both the Hamiltonian and the dissipation

$$X = -h^{\mathrm{T}} - \mathrm{i}\left(M_{\mathrm{g}} + M_{\mathrm{l}}^{\mathrm{T}}\right). \tag{10}$$

CPB Online In-Press

Similar to the classical damped-oscillation case, the time evolution of states in an open system also follows a damped-oscillation process. The dynamical details within damped oscillations are generally characterized by the Liouville spectrum, i.e., the eigenvalue spectrum of the damping matrix X in the complex plane denoted by $\{\lambda_n\}$. The imaginary parts of λ determine the rate at which the initial state converges to the steady state, and the smaller $\mathrm{Im}(\lambda)$ corresponds to faster convergence of the system to the steady state. Two special modes exist in the Liouvillian spectrum: one is the EDSs whose imaginary parts vanish, namely, $\mathrm{Im}(\lambda)=0$. The other is edge zero-frequency modes whose real parts vanish, i.e., $\mathrm{Re}(\lambda)=0$. Similar to the gapless edge mode corresponding to the Hamiltonian's topology, the EDSs and edge zero-frequency mode in dissipative dynamics are also related to the topology of the damping matrix.

Based on the Chern insulator of the Haldane model, we consider three particular types of dissipators to get the two special modes as

$$T_y: L_j^{\mathrm{g}}=\sqrt{\frac{\xi_{\mathrm{g}}}{2}}\left(c_{j,A}^{\dagger}+\mathrm{i}c_{j,B}^{\dagger}\right),\quad L_j^{\mathrm{l}}=\sqrt{\frac{\xi_{\mathrm{l}}}{2}}\left(c_{j,A}-\mathrm{i}c_{j,B}\right), \tag{11}$$

$$T_x: L_j^{\mathrm{g}}=\sqrt{\frac{\xi_{\mathrm{g}}}{2}}\left(c_{j,A}^{\dagger}+c_{j,B}^{\dagger}\right),\quad L_j^{\mathrm{l}}=\sqrt{\frac{\xi_{\mathrm{l}}}{2}}\left(c_{j,A}+c_{j,B}\right), \tag{12}$$

$$T_z: L_j^{\mathrm{g}}=\sqrt{\xi_{\mathrm{g}}}c_{j,A}^{\dagger},\ L_j^{\mathrm{l}}=\sqrt{\xi_{\mathrm{l}}}c_{j,A}, \tag{13}$$

where the subscript j represents the position of the unit cell. The coefficients ξ_{g} and ξ_{l} represent the coupling strength with the environment. For the case of T_y and T_x, the dissipation occurs on the A and B sublattices, while the dissipation only occurs on the A sublattice for case T_z. Then, the corresponding damping matrix of the dissipative Haldane model can be written as

$$X_{\mathrm{H}}^{y}(\boldsymbol{k})=-\left[\tilde{\xi}I+h_x\sigma_x+(h_y+\mathrm{i}\xi)\,\sigma_y-h_z\sigma_z\right], \tag{14}$$

$$X_{\mathrm{H}}^{x}(\boldsymbol{k})=-\left[\tilde{\xi}I+(h_x+\mathrm{i}\xi)\,\sigma_x+h_y\sigma_y-h_z\sigma_z\right], \tag{15}$$

$$X_{\mathrm{H}}^{z}(\boldsymbol{k})=-\left[\tilde{\xi}I+h_x\sigma_x+h_y\sigma_y-(h_z-\mathrm{i}\xi)\,\sigma_z\right], \tag{16}$$

with $\tilde{\xi}=\mathrm{i}\xi+h_0$ and $\xi=\frac{\xi_{\mathrm{g}}+\xi_{\mathrm{l}}}{2}$, and the corresponding Liouville spectra are

$$\lambda_{\mathrm{H}}^{y}(\boldsymbol{k})=-\tilde{\xi}\pm\sqrt{h_x^2+(h_y+\mathrm{i}\xi)^2+h_z^2}, \tag{17}$$

$$\lambda_{\mathrm{H}}^{x}(\boldsymbol{k})=-\tilde{\xi}\pm\sqrt{(h_x+\mathrm{i}\xi)^2+h_y^2+h_z^2}, \tag{18}$$

$$\lambda_{\mathrm{H}}^{z}(\boldsymbol{k})=-\tilde{\xi}\pm\sqrt{h_x^2+h_y^2+(h_z-\mathrm{i}\xi)^2}. \tag{19}$$

Now, in the Liouville spectrum, the modes with negative imaginary part ($\mathrm{Im}(\lambda)<0$) are allowed and will decay with time. However, the modes with positive imaginary part ($\mathrm{Im}(\lambda)>0$) are forbidden due to the fact that they increase with time. To investigate the topological properties of the dissipative Haldane model on the honeycomb lattice, we numerically study the Liouville spectra of damping matrices as defined in Eqs. (14)–(16) under a cylinder geometry. See the results in Figs. 1(a)–1(c). We have chosen armchair edges (y-direction) for periodic boundary conditions (PBC) and zigzag edges (x-direction) for open boundary conditions (OBC) in our cylinder geometric configuration.

Under OBC, the EDSs and edge zero-frequency mode exist in the topological region $\left(3\sqrt{3}t'>m\right)$ marked by the green or blue points in Figs. 1(a)–1(c). The EDSs exist only in the model with the T_y type dissipator under OBC along the zigzag edge as marked by the green points in Fig. 1(a). Remarkably, in the dissipative Haldane model, the emergence of imaginary and real line-gap closures in the edge states (including EDSs and edge zero-frequency mode) is attributed to the presence of a non-zero Chern number of the Haldane model. This reveals that the emergent edge states in the non-Hermitian Haldane model serve as dynamical indicators of its intrinsic topological characteristics. Figures 1(d)–1(f) present the distribution of edge modes of damping matrices in Eqs. (14)–(16). The EDSs are localized at the left edge of the system as in Fig. 1(d). In Fig. 1(f), due to the dissipation applied solely to the A sublattice under the T_z type dissipator in Eq. (13), the edge modes exhibit asymmetric localization at the two edges.

We can elucidate the physical origin of the edge dark states shown in Fig. 1(d) by examining the explicit form of the chiral edge states in the Haldane model. If the Haldane model is in a topological phase and PBCs are applied in the armchair edges (y-direction), chiral edge states with opposite chirality emerge on the left and right boundaries along the zigzag edges (x-direction), which are

$$\phi_{\mathrm{L}}\propto \mathrm{e}^{\mathrm{i}k_y y}\begin{pmatrix}1\\ i\end{pmatrix},\ \phi_{\mathrm{R}}\propto \mathrm{e}^{\mathrm{i}k_y y}\begin{pmatrix}1\\ -\mathrm{i}\end{pmatrix}. \tag{20}$$

Here, ϕ_{L} and ϕ_{R} are the chiral edge states localized at the left and right zigzag edges, 1 and the imaginary number i are the pseudo-spinor components of the sublattices. The dissipative Lindblad operator of T_y introduces coherent pairs $(1,\mathrm{i})^{\mathrm{T}}$ between internal degrees of freedom A and B in each unit cell. Consequently, the left edge modes, whose relative phase aligns with the coherent pair $(1,\mathrm{i})^{\mathrm{T}}$, remain unaffected by the environment and become the edge dark states (EDSs) of the system. In contrast, the right edge modes, whose relative phase is orthogonal to $(1,\mathrm{i})^{\mathrm{T}}$, are not supported within the system and are thus dissipated. Therefore, the EDSs are identified as the left edge modes of the Haldane model. We will study the topological protection in Subsection 2.2.

The damping matrix X fully characterizes the system's dissipative dynamics. To this end, we can examine the relaxation rate of the initial states toward the steady state. In our

CPB Online In-Press

analysis, the initial state corresponds to the scenario where all quantum states are fully occupied $C_0 = I$. Subsequently, the system is coupled to a Markovian environment, driving it toward a steady state characterized by the single-particle correlation function C_s. The deviation of the single-particle correlation function $C(t)$ from its steady state, denoted as $\tilde{C}(t) = C(t) - C_s$, obeys the time evolution equation: $\mathrm{i}\frac{\mathrm{d}}{\mathrm{d}t}\tilde{C} = X\tilde{C} - \tilde{C}X^\dagger$. The solution to this dynamical equation is

$$\begin{aligned}\tilde{C}(t) &= \mathrm{e}^{-\mathrm{i}Xt}\tilde{C}_0\,\mathrm{e}^{\mathrm{i}X^\dagger t} \\ &= \sum_{m,n}\mathrm{e}^{\mathrm{i}(-\lambda_n+\lambda_m^*)t}|u_n^{\mathrm{R}}\rangle\langle u_n^{\mathrm{L}}|\tilde{C}_0|u_m^{\mathrm{L}}\rangle\langle u_m^{\mathrm{R}}|, \end{aligned} \tag{21}$$

where $[\lambda_n]$ are the eigenvalues (or Liouville spectrum) of the damping matrix X, i.e., $X|u_n^{\mathrm{R}}\rangle = \lambda_n|u_n^{\mathrm{R}}\rangle$, $X^\dagger|u_n^{\mathrm{L}}\rangle = \lambda_n^*|u_n^{\mathrm{L}}\rangle$, where $|u_n^{\mathrm{R}}\rangle$ and $|u_n^{\mathrm{L}}\rangle$ are biorthogonal basis vectors and satisfy $\langle u_n^{\mathrm{L}}|u_m^{\mathrm{R}}\rangle = \delta_{mn}$. Equation (21) characterizes the damped oscillatory process of the system from the initial state C_0 to its steady state. Consequently, the non-Hermitian damping matrix X encodes the topological characteristics of the dissipative dynamics.

The time evolution of the on-site particle number $n_x(t)$ is characterized by $n_x = \tilde{C}_{xx}$, where x is the lattice site. Numerical results are presented in Figs. 1(g)–1(i). Comparing these three scenarios, the presence of edge dark states in the Liouvillian spectrum leads to spatial dependence in $n_x(t)$. During the time evolution, the decay behavior of $n_x(t)$ progressively transitions from exponential to non-decaying steady states when moving outward from the vicinity of the dark state boundary shown in Fig. 1(g). While in the trivial phase, the absence of an edge dark state leads to sustained exponential decay of $n_x(t)$. The stark contrast to the decay behavior in topologically non-trivial phases establishes the chirality-interrupted damping oscillations as a dynamical fingerprint for identifying topological order.

With the T_x type dissipator of Eq. (12), there may exist quasi-dark states due to $\mathrm{Im}[\lambda_{\mathrm{H}}^x(\boldsymbol{k})] \approx 0$ at the top of the valence band and the bottom of the conduction band, which may cause the time evolution of $n_x(t)$ to approach a steady state in the long-time limit like Fig. 1(h). However, for the T_z type dissipator in Eq. (13), the time evolution of $n_x(t)$ follows an exponentially decaying profile due to $\mathrm{Im}[\lambda_{\mathrm{H}}^z(\boldsymbol{k})] < 0$ shown in Fig. 1(i).

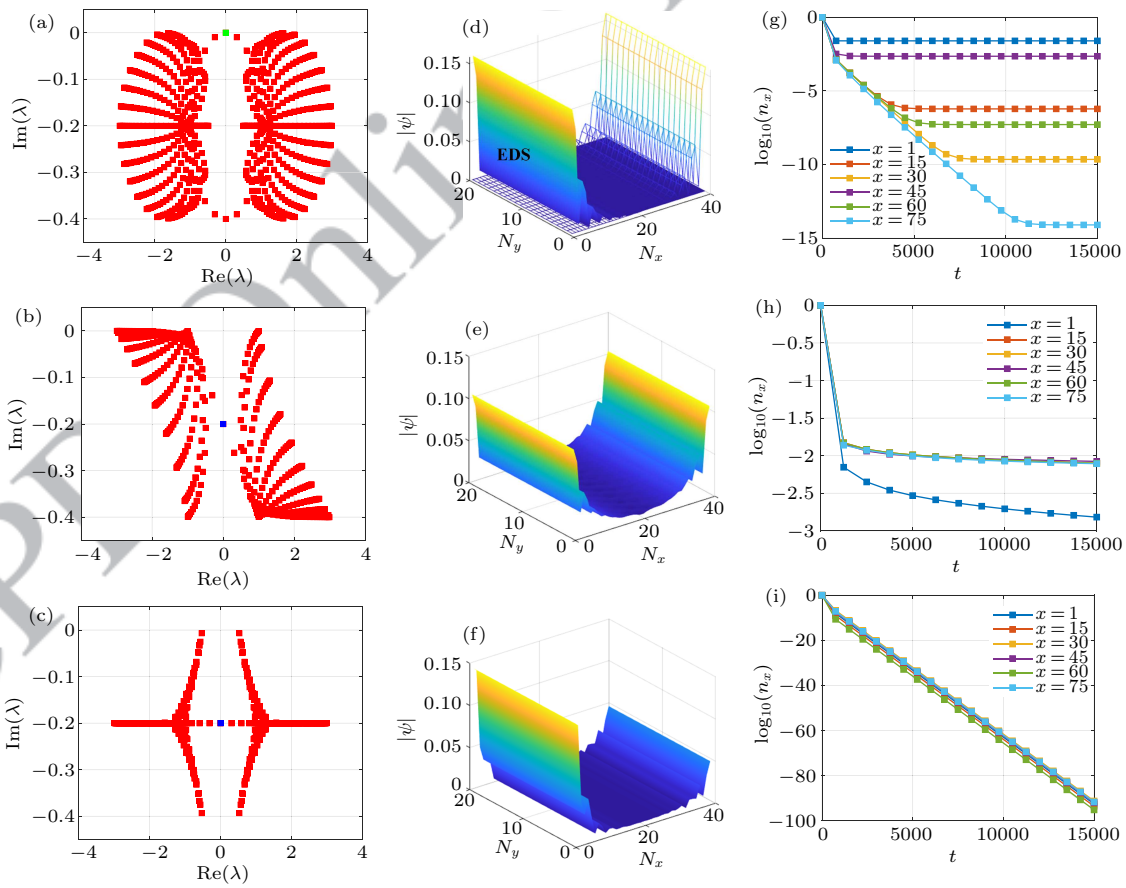


Fig. 1. (a)–(c) The Liouville spectra of the dissipative Haldane model under PBC in armchair edges (y-direction) and OBC in zigzag edges (x-direction) with different damping matrices as defined in Eqs. (14)–(16), respectively. The edge zero-frequency modes are labeled in blue points and the EDSs are labeled in green points. (d)–(f) The distribution of edge modes of damping matrices in Eqs. (14)–(16), respectively. The edge dark state (EDS) localized at the left edge of the system shown in (d). (g)–(i) The time evolution of the on-site particle number $n_x(t)$. $x = 1, 15, 30, 45, 60, 75$ are the global lattice-site indices in the $N_x \times N_y$ lattice. (a), (d) and (g) correspond to type-T_y dissipator in Eq. (11); (b), (e) and (h) correspond to type-T_x dissipator in Eq. (12); (c), (f) and (i) correspond to type-T_z dissipator in Eq. (13). The parameters are $t = 1$, $t' = 0.2$, $m = 0$, $\xi_{\mathrm{g}} = \xi_{\mathrm{l}} = 0.2$, $N_x = 40$, $N_y = 20$.

CPL Online First

2.2. The double damping matrix

The dark state in an open system refers to the mode that is decoupled from the environment. This state has a zero imaginary part in the Liouville spectrum and is often referred to as the non-decoherence subspace in the system.[39] A common method for constructing edge dark states is to neglect the original Hamiltonian and then build non-decoherence subspaces using specific Lindblad operators.[46] However, these edge dark states are prone to failure due to interference from the original Hamiltonian and the lack of topological protection. Nevertheless, in the above study, we have discovered that edge dark states can also exist in open systems that consist of the original Hamiltonian ($H \neq 0$), and they are localized at the edge of the system as in Figs. 1(a) and 1(d).

In topological band theory, the emergence of gapless edge modes that induce band-gap closure implies the existence of a nontrivial topological bulk gap. However, the modes with a positive imaginary part ($\mathrm{Im}(\lambda) > 0$) are forbidden in the Liouville spectrum. Furthermore, the above study indicates that EDSs are edge modes ($\mathrm{Im}(\lambda_{\mathrm{H}}^{y}) = 0$) protected by the topology of the damping matrix in Eq. (14). This implies that if the EDSs are protected by the topology of the dissipative Haldane model, it necessitates the existence of an imaginary energy gap, such that the imaginary parts of the energy bands exhibit opposite signs.

The damping matrix $X_{\mathrm{H}}^{y}(\boldsymbol{k})$ preserves the symmetry $\sigma_z X_{\mathrm{H}}^{y*}(-\boldsymbol{k})\sigma_z = -X_{\mathrm{H}}^{y}(\boldsymbol{k})$, which corresponds to the particle–hole symmetry of Hermitian systems. This implies that under open boundary conditions, there exist edge modes in the system. In these two chiral edge states that close the real energy gap, one of them also serves as an edge dark state when non-Hermiticity is introduced. To explore the topological protection of EDSs, we construct a double damping matrix by combining X and its complex conjugate X^*, i.e.,

$$\widetilde{X} = \begin{pmatrix} X_{\mathrm{H}}^{y} & 0 \\ 0 & X_{\mathrm{H}}^{y*} \end{pmatrix}. \tag{22}$$

Here, we have not considered the physical constraints on the Liouville spectrum, but rather treated them as a purely mathematical structure to analyze the relationship between its symmetries and edge dark states. Through numerical calculations under PBC, both the positive and negative imaginary parts are present in the spectra of $\widetilde{X}$ as in Fig. 2(a). The imaginary line gap of the non-Hermitian matrix $\widetilde{X}$ can be obtained as $\Delta E_{\mathrm{im}} = 2\max(\mathrm{Im}(\lambda_{\mathrm{H}}^{y}))$. It corresponds to the dynamics of the Liouville spectrum. We next calculate the Liouville spectrum of the double-damping matrix under OBC along the zigzag direction and discover the presence of edge dark states within the imaginary line gap marked by the green points in Fig. 2(b).

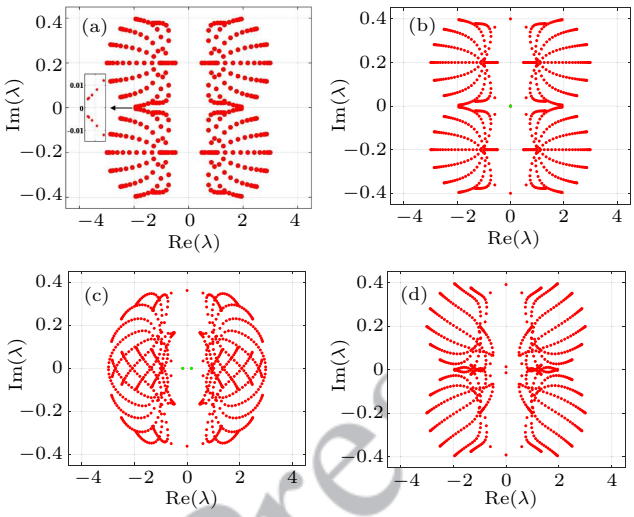


Fig. 2. (a) and (b) The Liouville spectra of the double damping matrix $\widetilde{X}$ under PBC and OBC along the zigzag direction, respectively. The EDSs are labeled in green. The parameters are $t = 1$, $t' = 0.2$, $m = 0$, $\xi_{\mathrm{g}} = \xi_{\mathrm{l}} = 0.2$, $N_x = 40$, $N_y = 10$. (c) and (d) The double Liouville spectrum given by the double damping matrix $\widetilde{X}_{\mathrm{H}}$ with perturbation coupling M_1 and M_2 under OBC along the zigzag direction, respectively. The EDSs are robust against the perturbation M_1 (c), while they are destroyed by the perturbation M_2 (d). The parameters are $c_1 = c_2 = 0.2$.

We then proceed to introduce perturbations into the double-damping matrix $\widetilde{X}$ in order to examine the robustness of the edge dark states. The double-damping matrix $\widetilde{X}$ inherently possesses time-reversal symmetry (TRS) and sublattice symmetry (SLS), i.e.,

$$\mathrm{TRS}: U_t \widetilde{X}^*(\boldsymbol{k}) U_t^{-1} = \widetilde{X}(-\boldsymbol{k}),$$
$$\mathrm{SLS}: U_s \widetilde{X}(\boldsymbol{k}) U_s^{-1} = -\widetilde{X}(\boldsymbol{k}).$$

Here, $U_t = \tau_x \otimes I$ or $\tau_y \otimes I$, and $U_s = \tau_x \otimes \sigma_z$ or $\tau_y \otimes \sigma_z$, where τ_x and τ_y act on the artificial degrees of freedom. It means that the symmetry classes of $\widetilde{X}$ are nonunique. However, an intriguing aspect is that the robustness of EDSs against perturbations is actually enhanced if the symmetry classes that give rise to nontrivial topology are not unique. To verify the robustness of EDSs, one can consider perturbations that correspond to the coupling between the degrees of freedom associated with X_{H}^{y} and X_{H}^{y*}. If the symmetry-consistent coupling can destroy the EDSs, then the corresponding topology is trivial. Conversely, if the EDSs exist in the presence of symmetry-consistent coupling, then the topological protection is nontrivial.

We introduce a double-damping matrix with perturbations defined as

$$\widetilde{X}_{\mathrm{H}} = \begin{pmatrix} X_{\mathrm{H}}^{y} & M \\ M^{\dagger} & X_{\mathrm{H}}^{y*} \end{pmatrix}. \tag{23}$$

The introduction of the coupling M may preserve or break the symmetry of the original double damping matrix $\widetilde{X}$. For instance, when $M = M^{\mathrm{T}}$, the TRS corresponding to $U_t = \tau_x \otimes I$ is preserved, while the TRS corresponding to $U_t = \tau_y \otimes I$ is broken. Conversely, when $M = -M^{\mathrm{T}}$, the TRS corresponding to $U_t = \tau_y \otimes I$ is preserved, whereas the TRS corresponding to

CPB Online First Preview

$U_t = \tau_x \otimes I$ is broken. In this work, we examine the symmetry-preserving perturbations defined as $M_1 = c_1 \cdot \tau_0 \otimes \sigma_x$ for $U_t = \tau_x \otimes I$, and $M_2 = c_2 \cdot \tau_0 \otimes \sigma_y$ for $U_t = \tau_y \otimes I$, c_1 and c_2 denote the perturbation strengths. The numerical results are shown in Figs. 2(c) and 2(d) under OBC along the zigzag direction. In Fig. 2(c), the EDSs are robust against the coupling M_1, whereas in Fig. 2(d), they are destroyed by the coupling M_2. This indicates that the EDSs are protected by the TRS of $U_t = \tau_x \otimes I$.

3. Edge dark states in a dissipative Kane–Mele model

The Kane–Mele model describes a two-dimensional topological insulator exhibiting the quantum spin Hall effect due to spin–orbit coupling, while preserving time-reversal symmetry.[1,47] In this section, we use similar methods to study the EDSs in a dissipative Kane–Mele model. Its Bloch Hamiltonian is given by

$$h_{\mathrm{KM}}(\boldsymbol{k}) = h_x I \otimes \sigma_x + h_y I \otimes \sigma_y + h_3 s_z \otimes \sigma_z,$$

under the basis vector $(c_{\boldsymbol{k}A\uparrow}, c_{\boldsymbol{k}B\uparrow}, c_{\boldsymbol{k}A\downarrow}, c_{\boldsymbol{k}B\downarrow})$, where $h_3 = -2\lambda_{\mathrm{so}}(-\sin\boldsymbol{k}\cdot\boldsymbol{a}_1 + \sin\boldsymbol{k}\cdot\boldsymbol{a}_2 + \sin\boldsymbol{k}\cdot\boldsymbol{a}_3)$, λ_{so} denotes the spin–orbit coupling strength, and Pauli matrices $s_{x,y,z}$ act on spin degrees of freedom. The model preserves the TRS, i.e., $U_t h^*_{\mathrm{KM}}(\boldsymbol{k}) U_t^{-1} = h_{\mathrm{KM}}(\boldsymbol{k})$ with $U_t = s_y \otimes I$. It is characterized by a Z_2 topological invariant and belongs to class AII in the ten-fold way classification of non-interacting topological states.

To ensure the existence of edge dark states in the dissipative Kane–Mele model, a finite Liouville gap should exist in the system. This requires that the non-Hermitian terms induced by the Markovian environment in the damping matrix anti-commute with the Hamiltonian $h_{\mathrm{KM}}(\boldsymbol{k})$. There exist four possible types of dissipators

$$\begin{aligned} T_1: L^{\mathrm{g}}_j &= \sqrt{\xi_{\mathrm{g}}}(c^\dagger_{j,A,\uparrow} + c^\dagger_{j,B,\uparrow}), \\ L^{\mathrm{l}}_j &= \sqrt{\xi_{\mathrm{l}}}(c_{j,A,\downarrow} + c_{j,B,\downarrow}), \end{aligned} \tag{24}$$

$$\begin{aligned} T_2: L^{\mathrm{g}}_j &= \sqrt{\xi_{\mathrm{g}}}(c^\dagger_{j,A,\uparrow} + \mathrm{i}c^\dagger_{j,B,\uparrow}), \\ L^{\mathrm{l}}_j &= \sqrt{\xi_{\mathrm{l}}}(c_{j,A,\downarrow} - \mathrm{i}c_{j,B,\downarrow}), \end{aligned} \tag{25}$$

$$\begin{aligned} T_3: L^{\mathrm{g}}_j &= \sqrt{\xi_{\mathrm{g}}}(c^\dagger_{j,A,\uparrow} + c^\dagger_{j,A,\downarrow}), \\ L^{\mathrm{l}}_j &= \sqrt{\xi_{\mathrm{l}}}(c_{j,B,\uparrow} - c_{j,B,\downarrow}), \end{aligned} \tag{26}$$

$$\begin{aligned} T_4: L^{\mathrm{g}}_j &= \sqrt{\xi_{\mathrm{g}}}(c^\dagger_{j,A,\uparrow} + \mathrm{i}c^\dagger_{j,A,\downarrow}), \\ L^{\mathrm{l}}_j &= \sqrt{\xi_{\mathrm{l}}}(c_{j,B,\uparrow} + \mathrm{i}c_{j,B,\downarrow}). \end{aligned} \tag{27}$$

The corresponding damping matrices of the dissipative Kane–Mele model are written as

$$\begin{aligned} X^1_{\mathrm{KM}}(\boldsymbol{k}) &= -\mathrm{i}\xi I \otimes I - (h_x + \mathrm{i}\xi) I \otimes \sigma_x \\ &\quad - h_y I \otimes \sigma_y + h_3 s_z \otimes \sigma_z, \end{aligned} \tag{28}$$

$$\begin{aligned} X^2_{\mathrm{KM}}(\boldsymbol{k}) &= -\mathrm{i}\xi I \otimes I - h_x I \otimes \sigma_x \\ &\quad - (h_y + \mathrm{i}\xi) I \otimes \sigma_y + h_3 s_z \otimes \sigma_z, \end{aligned} \tag{29}$$

$$\begin{aligned} X^3_{\mathrm{KM}}(\boldsymbol{k}) &= -\mathrm{i}\xi I \otimes I - h_x I \otimes \sigma_x - h_y I \otimes \sigma_y \\ &\quad + h_3 s_z \otimes \sigma_z - \mathrm{i}\xi s_x \otimes \sigma_z, \end{aligned} \tag{30}$$

$$\begin{aligned} X^4_{\mathrm{KM}}(\boldsymbol{k}) &= -\mathrm{i}\xi I \otimes I - h_x I \otimes \sigma_x - h_y I \otimes \sigma_y \\ &\quad + h_3 s_z \otimes \sigma_z - \mathrm{i}\xi s_y \otimes \sigma_z. \end{aligned} \tag{31}$$

Numerical calculations show that in the topological phase of the Kane–Mele model with PBC in the armchair direction and OBC in the zigzag direction, the T_1 type dissipator induces edge zero-frequency states, while the $T_{2,3,4}$ type dissipator leads to the emergence of EDSs, as shown in Fig. 3. We find that the damping matrix $X^2_{\mathrm{KM}}(\boldsymbol{k})$ with dissipator T_2 shares the same symmetry with $X^y_{\mathrm{H}}(\boldsymbol{k})$ in Eq. (14), namely, $s_z \otimes \sigma_z X^{2*}_{\mathrm{KM}}(-\boldsymbol{k}) s_z \otimes \sigma_z = -X^2_{\mathrm{KM}}(\boldsymbol{k})$. This suggests that their corresponding doubled damping matrices share the same topological properties. The EDSs are topologically protected and robust. Moreover, under the T_2 type dissipator, as long as the introduction of on-site staggered potential m does not destroy the topological phase of the Kane–Mele model, the EDSs will always remain present.

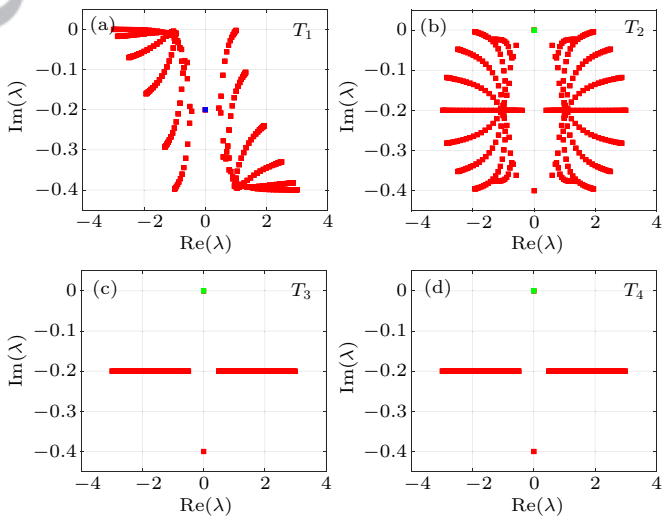


Fig. 3. The Liouville spectra of the dissipative Kane–Mele model with different dissipators under PBC in the armchair direction and OBC in the zigzag direction on a honeycomb lattice. (a) is a T_1 type of dissipator; (b) is a T_2 type of dissipator; (c) is a T_3 type of dissipator and (d) is a T_4 type of dissipator. The edge dark states are labeled in green. The parameters are $t = 1$, $\lambda_{\mathrm{so}} = 0.1$, $\xi_{\mathrm{g}} = \xi_{\mathrm{l}} = 0.2$, $N_x = 40$, $N_y = 10$.

There exists time-reversal symmetry similar to that in the Hermitian system for the damping matrices $X^3_{\mathrm{KM}}(\boldsymbol{k})$ and $X^4_{\mathrm{KM}}(\boldsymbol{k})$ in Eqs. (30) and (31), i.e.,

$$I \otimes \sigma_z \cdot X^{3*}_{\mathrm{KM}}(-\boldsymbol{k}) \cdot I \otimes \sigma_z = -X^3_{\mathrm{KM}}(\boldsymbol{k}), \tag{32}$$

$$s_z \otimes \sigma_z \cdot X^{4*}_{\mathrm{KM}}(-\boldsymbol{k}) \cdot s_z \otimes \sigma_z = -X^4_{\mathrm{KM}}(\boldsymbol{k}). \tag{33}$$

As illustrated in Figs. 3(c) and 3(d), the edge dark states close the point gap in their corresponding double damping ma-

CPB Online In-Press

trices $\widetilde{X}^i_{\rm KM} = \begin{pmatrix} X^i_{\rm KM} & 0 \\ 0 & X^{i*}_{\rm KM} \end{pmatrix}$, where $i = 3$ or 4 represents different dissipators. Similarly, to verify the topological protection and robustness of the edge dark states, we introduce two types of perturbations in the double-damping matrix for testing, namely, $M_{\rm km1} = c_3 \cdot I \otimes I \otimes \sigma_x$ and $M_{\rm km2} = c_4 \cdot I \otimes I \otimes \sigma_z$; c_3 and c_4 denote the perturbation strengths. The numerical results, presented in Fig. 4, demonstrate that in the Kane–Mele model, if the T_3 or T_4 type of dissipator is introduced, the perturbation $M_{\rm km2}$ would disrupt the edge dark states, while the perturbation $M_{\rm km1}$ leaves them unaffected. In addition, under either T_3 or T_4 type dissipator conditions, the presence of an on-site staggered potential m removes the EDSs in all cases.

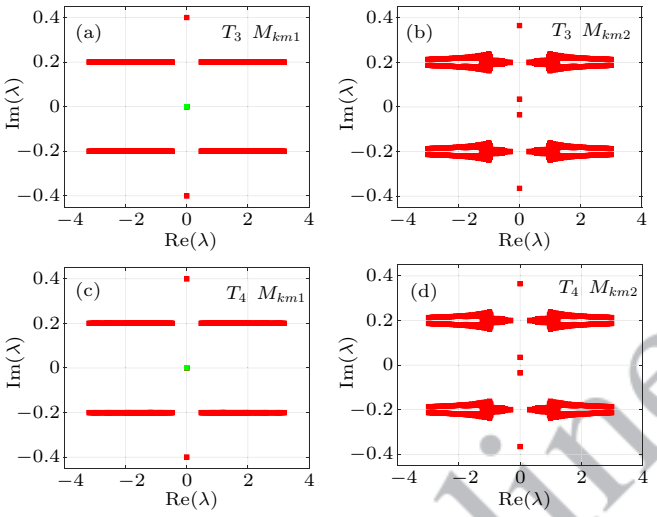


Fig. 4. The Liouville spectra of a double damping matrix in a dissipative Kane–Mele model with OBC in the zigzag direction. (a) and (b) are the double damping matrices under a T_3 type dissipator with perturbations $M_{\rm km1}$ and $M_{\rm km2}$, respectively. (c) and (d) are the double damping matrices under a T_4 type dissipator with perturbations $M_{\rm km1}$ and $M_{\rm km2}$, respectively. The EDSs are marked by green. EDSs are robust against the perturbation $M_{\rm km1}$, while they are destroyed by the perturbation $M_{\rm km2}$. The parameters are $t = 1$, $\lambda_{\rm so} = 0.1$, $\xi_{\rm g} = \xi_{\rm l} = 0.2$, $N_x = 40$, $N_y = 10$, $c_3 = c_4 = 0.2$.

4. Discussion and conclusion

In this work, we investigate the edge dark states in a dissipative Haldane model and a dissipative Kane–Mele model within an open quantum system framework that incorporates both Hamiltonian dynamics and dissipative effects. For a given dissipator $L^{\rm g,l}_j$, we derive a non-Hermitian damping matrix X from the time evolution equation for the single-particle correlation functions, where the dynamical details of damped oscillations are generally characterized by the Liouvillian spectrum of X. Through numerical simulations, we demonstrate the existence of topologically protected edge zero-frequency modes and edge dark states. In the topological phase, the edge zero-frequency modes are progressively suppressed as the dissipation strength $\xi_{\rm g,l}$ increases. The time evolution of the occupation numbers reveals that the edge dark states lead to chirality interruption in damped oscillatory dynamics.

In summary, previous studies have established that edge dark states can arise in purely dissipative systems, and it was commonly believed that the introduction of a Hamiltonian would typically disrupt the topological protection of these states. However, our work reveals that the robustness of EDSs originates from their topological nature, which persists even in the presence of the Hamiltonian. Further studies involving perturbations showed that the edge dark states can maintain their stability as long as the perturbations do not destroy the imaginary line gap. The edge dark states are robust and topologically protected by the double damping matrix.

Acknowledgements

This work is supported by National Natural Science Foundation of China (Grant Nos. 11404090, 11304136, and 12275203), the Science Foundation for Youth Top-notch Talent of Hebei Education Department (Grant No. BJ2018053), Distinguished Young Scholar Fund of Hebei Normal University, and the Scientific Research Program Funded by the Natural Science Basic Research Plan in Shaanxi Province of China (Grant No. 2021JM-421).

References

[1] Kane C L and Mele E J 2005 *Phys. Rev. Lett.* **95** 226801
[2] Bernevig B A, Hughes T L and Zhang S C2006 *Science* **314** 1757
[3] König M, Wiedmann S, Brüne C, Roth A, Buhmann H, Molenkamp L W, Qi X L and Zhang S C 2007 *Science* **318** 766
[4] Hasan M Z and Kane C L 2010 *Rev. Mod. Phys.* **82** 3045
[5] Zhou Y C, Yu J L, Chen Y H, Lai Y F and Cheng S Y 2023 *Chin. Phys. B* **32** 087102
[6] Kitaev A Yu 2001 *Phys. Usp.* **44** 131
[7] Fu L and Kane C L 2008 *Phys. Rev. Lett.* **100** 096407
[8] Mourik V, Zuo K, Frolov S M, Plissard S R, Bakkers E P A M and Kouwenhoven L P 2012 *Science* **336** 1003
[9] Alicea J 2012 *Rep. Prog. Phys.* **75** 076501
[10] Wen X G 1990 *Int. J. Mod. Phys. B* **4** 239
[11] Kitaev A Yu 2003 *Ann. Phys.* **303** 2
[12] Han T H, Helton J S, Chu S, Nocera D G, Rodriguez-Rivera J A, Broholm C and Lee Y S 2012 *Nature* **492** 406
[13] Nayak C, Simon S H, Stern A, Freedman M and Das Sarma S D 2008 *Rev. Mod. Phys.* **80** 1083
[14] Benalcazar W A, Bernevig B A and Hughes T L 2017 *Science* **357** 61
[15] Benalcazar W A, Bernevig B A and Hughes T L 2017 *Phys. Rev. B* **96** 245115
[16] Schindler F, Cook A M, Vergniory M G, Wang Z, Parkin S S P, Bernevig B A and Neupert T 2018 *Sci. Adv.* **4** eaat0346
[17] Langbehn J, Peng Y, Trifunovic L, von Oppen F and Brouwer P W 2017 *Phys. Rev. Lett.* **119** 246401
[18] Wang Q and Hao N 2024 *Chin. Phys. B* **33** 127303
[19] Shen Y F, Xu X F, Sun M, Zhou W J and Chang Y J 2024 *Chin. Phys. B* **33** 044203
[20] Fu L 2011 *Phys. Rev. Lett.* **106** 106802
[21] Tanaka Y, Ren Z, Sato T, Nakayama K, Souma S, Takahashi T, Segawa K and Ando Y 2012 *Nat. Phys.* **8** 800
[22] Qi X L and Zhang S C 2011 *Rev. Mod. Phys.* **83** 1057
[23] Weimann S, Kremer M, Plotnik Y, Lumer Y, Nolte S, Makris K G, Segev M, Rechtsman M C and Szameit A 2017 *Nat. Mater.* **16** 433
[24] Zeuner J M, Rechtsman M C, Plotnik Y, Lumer Y, Nolte S, Rudner M S, Segev M and Szameit A 2015 *Phys. Rev. Lett.* **115** 040402
[25] Bender C M and Boettcher S 1998 *Phys. Rev. Lett.* **80** 5243
[26] Rüter C E, Makris K G, El-Ganainy R, Christodoulides D N, Segev M and Kip D 2010 *Nat. Phys.* **6** 192
[27] Heiss W D 2004 *J. Phys. A: Math. Gen.* **37** 2455

CPB Online In Press

[28] Yao S Y and Wang Z 2018 *Phys. Rev. Lett.* **121** 086803
[29] Song F, Yao S Y and Wang Z 2019 *Phys. Rev. Lett.* **123** 170401
[30] Kunst F K, Edvardsson E, Budich J C and Bergholtz E J 2018 *Phys. Rev. Lett.* **121** 026808
[31] Yokomizo K and Murakami S 2019 *Phys. Rev. Lett.* **123** 066404
[32] Ashida Y, Gong Z P and Ueda M 2020 *Adv. Phys.* **69** 249
[33] Bergholtz E J, Budich J C and Kunst F K 2021 *Rev. Mod. Phys.* **93** 015005
[34] Dangel F, Wagner M, Cartarius H, Main J and Wunner G 2018 *Phys. Rev. A* **98** 013628
[35] Gneiting C, Koottandavida A, Rozhkov A V and Nori F 2022 *Phys. Rev. Res.* **4** 023036
[36] Cheng J, Zhang X, Lu M H and Chen Y F 2022 *Phys. Rev. B* **105** 094103
[37] van Caspel M T, Arze S E T and Castillo I P 2019 *SciPost Phys.* **6** 026
[38] Lieu S, McGinley M and Cooper N R 2020 *Phys. Rev. Lett.* **124** 040401
[39] Diehl S, Rico E, Baranov M A and Zoller P 2011 *Nat. Phys.* **7** 971
[40] Bardyn C E, Baranov M A, Kraus C V, Rico E, Imamoglu A, Zoller P and Diehl S 2013 *New J. Phys.* **15** 085001
[41] Haldane F D M 1988 *Phys. Rev. Lett.* **61** 2015
[42] Lindblad G 1976 *Commun. Math. Phys.* **48** 119
[43] Gorini V, Kossakowski A and Sudarshan E C G 1976 *J. Math. Phys.* **17** 821
[44] Wolf M and Cirac J I 2008 *Commun. Math. Phys.* **279** 147
[45] Breuer H P and Petruccione F 2002 *The Theory of Open Quantum Systems* (Oxford: Oxford University Press) p. 2
[46] Shavit G and Goldstein M 2020 *Phys. Rev. B* **101** 125412
[47] Kane C L and Mele E J 2005 *Phys. Rev. Lett.* **95** 146802

CPB Online In-Press